

# A Novel High Bandwidth Efficiency Interference Alignment Scheme Based on Continuous Phase Modulation

Zhilu Wu<sup>1</sup>, Lihui Jiang<sup>1</sup>, Guanghui Ren<sup>1</sup>, and Gangyi Wang<sup>2</sup>

<sup>1</sup>School of Electronics and Information Engineering, Harbin Institute of Technology, Harbin, 150001, China

<sup>2</sup>School of Instrumentation Science and Opto-Electronics Engineering, Beihang University, Beijing 100191, China

Email: {wuzhilu; jianglihui; rgh}@hit.edu.cn; WangGangyi@buaa.edu.cn

**Abstract**—Interference alignment (IA) is an emerging technique which can suppress the interference effectually and provides a means to approach the channel capacity in the multiple-input and multiple-output (MIMO) networks. However, little work has concentrated on the bandwidth efficiency of IA systems, which is undoubtedly important especially in the current situations of spectrum scarcity. In this paper, a novel IA scheme is proposed, which leverages the advanced continuous phase modulation (CPM) to increase the bandwidth efficiency. Due to the continuity of the information-bearing phase, the proposed CPM-IA scheme exhibits low sidelobe and rapid spectrum rolloff. Moreover, a low-complexity pulse amplitude modulated (PAM) decomposition algorithm is applied to CPM-IA scheme, which can reduce the number of matched filters without much performance degradation. In addition, a novel spatial-frequency domain (SFD)-CPM-IA scheme is proposed to mitigate the interference that the traditional IA cannot handle when the IA feasibility condition cannot be satisfied. The proposed SFD-CPM-IA scheme inherits the high bandwidth efficiency of CPM-IA, and can accommodate many more users to communicate simultaneously.

**Index Terms**—Interference alignment, bandwidth efficiency, continuous phase modulation, pulse amplitude modulated (PAM) decomposition, spatial-frequency domain, bit error rate (BER)

## I. INTRODUCTION

Interference alignment (IA) technique has attracted a great deal of attention for its ability of eliminating the interferences and increasing the throughput of modern wireless communication systems, where the demand for high data rate transmission has increased considerably in recent years. The degrees of freedom (DoFs) of IA networks have been studied in [1] and proved to be proportional to the number of users in the high signal-to-noise ratio (SNR) regimes. In the IA system, proper precoding matrices are designed to cast the interferences and desired signals into different signal subspaces. Consequently, when the corresponding decoding matrices are exerted on the received signals, the intended signals can be reconstructed with low undesired interference leakage [2]. The closed-form solutions of IA can be formulated only in certain scenarios and general analytical solutions remain unknown [3]. An alternating

minimization interference leakage (AMinIL) algorithm was proposed in [4], where the channel reciprocity is taken into consideration and the near IA points can be approached. However, AMinIL algorithm does not take the desired signal into account, and its sum rate achievement is not optimal. Therefore, Gomadam *et al.* turned to maximize the signal-to-interference-plus-noise ratio (SINR), and proposed the Max-SINR algorithm [5], which can achieve higher throughput. The relationship between IA and other transceiver design strategies has been investigated by Lu *et al.* [6]. In addition, traditional IA systems are based on the knowledge of perfect channel state information (CSI), which is difficult to obtain in the practical systems. Therefore, many researchers have focused on the IA networks with imperfect CSI. Ayach *et al.* [7] have proposed a CSI training and feedback mechanism to maximize the effective sum rate. The performance of IA is studied in [8], where the CSI is fed back through limited bits, and a new IA scheme is proposed to mitigate this problem. In addition, Zhao *et al.* have conducted a review on the Opportunistic Communications based IA in [9], and proposed a simultaneous wireless information and power transfer scheme to improve the quality of service (QoS) of IA networks. Due to the significant advantages, IA has been applied to the relay networks [10], [11], cognitive radio [12], [13], and green communications [14], [15].

To the best of our knowledge, most of the existed works on IA mainly focus on increasing the DoFs and sum rate, while little work concentrates on the bandwidth efficiency. It is well known that the contradiction between the upgrading demand for high data rate communication and the limited usable radio resource is becoming more and more serious. Consequently, many strategies have been proposed to mitigate the problem of spectrum scarcity, such as spectrum-sharing [16] and cognitive radio [17]. Therefore, the high bandwidth efficiency IA scheme is demanded. In this paper, we concentrate on increasing the bandwidth efficiency of IA networks by introducing the advanced continuous phase modulation (CPM). Different from the traditional binary phase shift keying (BPSK) modulation which is used in current IA networks [18], the phase of CPM signal changes continuously. Therefore, the associated signal has sharper spectrum rolloff and lower bandwidth [19]. Particularly, the exceptional property of constant

---

Manuscript received January 21, 2015; revised April 13, 2015.

Corresponding author email: wuzhilu@hit.edu.cn.

doi:10.12720/jcm.10.4.268-275

envelopmake it suitable to mitigate the distortion caused by the non-linear amplifier [20]. In addition, the memory inherent in the phase provides extra coding gain compared with the symbol-by-symbol detection. Due to its promising performance, CPM has been applied to spread spectrum system [21], satellite communications [22], fiber-optic links [23] *et al.* Particularly, Multi-h CPM, which is an important variance of CPM, has been adopted as the aeronautical telemetry standard by the US military [24]. Therefore, the proposed CPM-IA scheme is expected to inherit the advantages of IA and CPM.

Due to the memory inherent in the phase, CPM cannot be demodulated symbol-by-symbol, and has to employ the trellis decoder such as the Viterbi algorithm (VA). However, traditional VA suffers from high computational cost with large number of match filters and trellis states. In the proposed CPM-IA scheme, such a problem still exists. Therefore, we develop a low complexity CPM-IA scheme based on decomposing the CPM signals into a series of pulse amplitude modulated (PAM) components and utilizing the major components to approximate the original signals.

Most of the previous works on IA were conducted under the IA feasibility condition, i.e.,  $K \leq (M+N)/d-1$ , where  $K$ ,  $M$ ,  $N$ , and  $d$  represent the numbers of users, transmitting antennas, receiving antennas, and DoFs, respectively. However, in the practical systems where the number of antennas is usually limited and a great many of users often transmit data simultaneously, the IA feasibility constraint cannot be met, and the interferences will no longer be aligned properly, leading to significantly degradation of the QoS. Although a clustering-IA was proposed in [25] to mitigate the interference, it cannot be applied to the traditional symmetric networks. Therefore, a novel spatial-frequency domain (SFD)-CPM-IA scheme is proposed, which jointly aligns the interferences into the spatial and frequency dimensions. In the proposed scheme, the large numbers of users are first divided into different groups, and the CPM-IA technique is applied to each cluster. Moreover, different groups are assigned with different frequencies, so that the inter-cluster interferences can be eliminated. Due to the narrow bandwidth of CPM-IA scheme, the frequency gap of the adjacent groups can be set to be small, and the total bandwidth of the whole system can be reduced. Therefore, the proposed SFD-CPM-IA scheme can not only eliminate the interferences which are beyond the ability of the traditional IA, but also increase the bandwidth efficiency of the large-scale networks.

The rest of this paper is organized as follows. Section II provides the IA system model. The CPM-IA scheme and the associated low complexity PAM decomposition algorithm are proposed in Section III. In Section IV, the SFD-CPM-IA scheme is developed. Simulations are conducted in Section V. Finally, we conclude the paper in Section VI.

Notations: We use  $(M \times N, d)^K$  to represent the multiple-input and multiple-output (MIMO) interference channel with  $K$  users, each of which is equipped with  $M$  transmitting antennas,  $N$  receiving antennas, and  $d$  DoFs.  $\mathbf{A}^T$ ,  $\mathbf{A}^H$ , and  $\mathbf{A}_{(l)}$  mean the transpose, the conjugate transpose, and the  $l$ th column of matrix  $\mathbf{A}$ , respectively.  $\mathbf{I}$ ,  $\mathbb{R}^{M \times N}$ , and  $\mathbb{C}^{M \times N}$  indicate the identity matrix, the  $M \times N$  real matrix, and the  $M \times N$  complex matrix, respectively.

## II. SYSTEM MODEL

As shown in Fig. 1, the  $(M \times N, d)^K$  interference channel is considered in this paper. The bit vector of the  $k$ th ( $k=1, 2, \dots, K$ ) user is given by

$$\mathbf{c}_k(n) = [c_{k,1}(n), c_{k,2}(n), \dots, c_{k,d}(n)]^T, n = 1, 2, 3, \dots \quad (1)$$

with

$$c_{k,l}(n) \in \{+1, -1\}, l = 1, 2, \dots, d \quad (2)$$

$\mathbf{c}_k(n)$  is firstly modulated by the modulator to generate the waveform vector  $\mathbf{s}_k(t) = [s_{k,1}(t), s_{k,2}(t), \dots, s_{k,d}(t)]^T \in \mathbb{C}^{d \times 1}$ . Notice that each data stream of  $\mathbf{c}_k(n)$  is modulated separately. The  $k$ th transmitter employs the precoding matrix  $\mathbf{P}_k \in \mathbb{C}^{M \times d}$  to process  $\mathbf{s}_k(t)$  so that the interferences and desired signals are aligned into different signal subspaces, and the associated transmitting signal vector can be given by:

$$\mathbf{X}_k(t) = \mathbf{P}_k \mathbf{s}_k(t) \quad (3)$$

At the  $k$ th receiver, the received signal vector can be expressed as:

$$\mathbf{Y}_k(t) = \sum_{j=1}^K \mathbf{H}_{kj} \mathbf{X}_j(t) + \mathbf{n}_k(t) \quad (4)$$

where  $\mathbf{H}_{kj}$  denotes the channel response matrix from transmitter  $j$  to receiver  $k$ ;  $\mathbf{n}_k(t)$  represents the zero-mean complex additive white Gaussian noise (AWGN) vector with variance of  $\sigma^2$ . Throughout this paper, ideal CSI is assumed to be perfectly known at each node. The receiver utilizes the decoding matrix  $\mathbf{D}_k$  to eliminate the interferences, and the reconstructed signal can be given by:

$$\hat{\mathbf{s}}_k(t) = [\hat{s}_{k,1}(t), \hat{s}_{k,2}(t), \dots, \hat{s}_{k,d}(t)]^T = \mathbf{D}_k^H \mathbf{Y}_k(t) \quad (5)$$

Finally,  $\hat{\mathbf{s}}_k(t)$  is demodulated and the final bit vector  $\hat{\mathbf{c}}_k(n)$  can be attained.

The interference-plus-noise covariance matrices of the  $l$ th data stream of user  $k$  in the forward and reciprocal channels can be respectively expressed as:

$$\mathbf{B}_{kl} = \sum_{j=1, j \neq k}^K \mathbf{H}_{kj} \mathbf{P}_j \mathbf{P}_j^H \mathbf{H}_{kj}^H + \sum_{r=1, r \neq l}^d \mathbf{H}_{kk} \mathbf{P}_{k(r)} \mathbf{P}_{k(r)}^H \mathbf{H}_{kk}^H + \sigma^2 \mathbf{I} \quad (6)$$

$$\bar{\mathbf{B}}_{kl} = \sum_{j=1, j \neq k}^K \mathbf{H}_{jk}^H \mathbf{D}_j \mathbf{D}_j^H \mathbf{H}_{jk} + \sum_{r=1, r \neq l}^d \mathbf{H}_{kk}^H \mathbf{D}_{k(r)} \mathbf{D}_{k(r)}^H \mathbf{H}_{kk} + \sigma^2 \mathbf{I} \quad (7)$$

The IA technique is to design proper precoding and decoding matrices so that the following conditions can be satisfied [5]:

$$\mathbf{D}_k^H \mathbf{H}_{kj} \mathbf{P}_j = \mathbf{0} \quad (8)$$

$$\text{rank}(\mathbf{D}_k^H \mathbf{H}_{kk} \mathbf{P}_k) = d \quad (9)$$

To the best of our knowledge, little existed work has focused on the bandwidth efficiency as well as the modulation scheme of IA systems, which are undoubtedly important in the practical applications. In the next section, we will propose a high bandwidth efficiency IA scheme by leveraging the advanced continuous phase modulation.

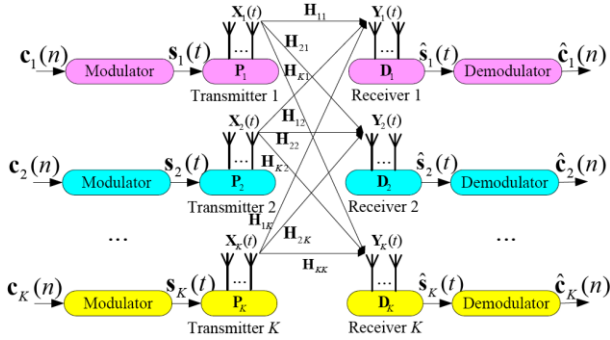


Fig. 1. The IA system model

### III. CONTINUOUS PHASE MODULATION IA SCHEME

Although the IA technique can mitigate the interferences effectively, the bandwidth of the traditional IA system which employs BPSK modulation is relatively wide, exacerbating the spectrum scarcity problem. In this section, a novel continuous phase modulation IA scheme is proposed, which can alleviate the bandwidth requirement significantly. Besides, the phase memory which is embedded in the modulated signal can be leveraged to further improve the error performance. Moreover, the constant envelope waveform property of the CPM-IA scheme provides extraordinary resistance to the nonlinear distortion caused by the front-end amplifier.

#### A. The Precoding/Decoding Matrices Design Strategy

In the CPM-IA scheme, the interferences from the unintended users are mitigated by the precoding matrices  $\mathbf{P}$  and the decoding matrices  $\mathbf{D}$ . However, the closed-form solution of the optimal  $\mathbf{P}$  and  $\mathbf{D}$  is still not available in most situations. Therefore, numerical methods are employed to design the suboptimal  $\mathbf{P}$  and  $\mathbf{D}$  under different criteria. In the IA systems, the CSI should be estimated at each receiver and then fed back to the transmitters. The CSI feedback will take extra frequency

bands, and will degrade the CSI at the transmitters, leading to undesired performance loss of the IA systems. The Max-SINR algorithm proposed in [5] has great advantages in that it only requires the local CSI at each node by leveraging the channel reciprocity of wireless networks. Moreover, it can achieve higher sum rate than many previous algorithms. Therefore, we choose the Max-SINR algorithm as the beamforming design strategy in the proposed CPM-IA scheme.

The procedure of Max-SINR algorithm can be summarized in Algorithm 1. During each iteration, the precoding matrices are firstly fixed, and the decoding matrices that maximize the SINR are formulated according to the 5th line. The same procedure is executed in the reciprocal channel by fixing the decoding matrices to attain the associated precoding matrices according to the 8th line. The Max-SINR algorithm can jointly optimize the desired signal and interferences, and hence can achieve good sum rate.

---

#### Algorithm 1: Max-SINR Algorithm

---

1. Initialize  $\mathbf{P}_k, k=1,2,\dots,K$ .  $\mathbf{P}_{k(l)}$  ( $l=1,2,\dots,d$ ) are linearly independent vectors with  $\|\mathbf{P}_{k(l)}\|=1$ .
  2. Initialize  $I_{\max}$ . Set  $i=0$ .
  3. **Repeat**
  4. Fixing  $\mathbf{P}_k$ , and calculate  $\mathbf{B}_{kl}$  according to (6).
  5. Calculate  $\mathbf{D}_k$  as:  

$$\mathbf{D}_{k(l)} = \mathbf{B}_{k(l)}^{-1} \mathbf{H}_{kk} \mathbf{P}_{k(l)}$$
  6. Normalize  $\mathbf{D}_{k(l)}$ .
  7. Fixing  $\mathbf{D}_k$  and calculate  $\bar{\mathbf{B}}_{kl}$  according to (7).
  8. Calculate the matrix  $\mathbf{P}_k$  as:  

$$\mathbf{P}_{k(l)} = \bar{\mathbf{B}}_{k(l)}^{-1} \mathbf{H}_{kk}^H \mathbf{D}_{k(l)}$$
  9. Normalize  $\mathbf{P}_{k(l)}$ .
  10.  $i=i+1$ ;
  11. **Until**  $i > I_{\max}$  or the algorithm converges.
- 

#### B. The Signal Waveform of CPM-IA Schemel

In the CPM-IA scheme, we employ the continuous phase modulation to increase the bandwidth and power efficiency. The equivalent base band signal of the  $l$ th data stream of the  $k$ th user can be expressed as:

$$s_{k,l}(t) = \sqrt{E/T} \exp\{\phi_{k,l}(t)\} \quad (10)$$

where  $E$ ,  $T$ , and  $\phi_{k,l}$  represent the symbol energy, symbol period, and the information-bearing phase, respectively. The relationship between the phase and bit stream can be depicted as:

$$\phi_{k,l}(t) = 2\pi h \sum_n c_{k,l}(n) q(t-nT) \quad (11)$$

where  $h$  and  $q(t)$  represent the modulation index and phase pulse function, respectively.  $q(t)$  is the integral of the frequency pulse function  $f(t)$ , which satisfies the following conditions:

$$f(t) = \begin{cases} f(t) & t \leq LT \\ 0 & t > LT \end{cases} \quad (12)$$

$$q(t) = \int_{-\infty}^t f(\tau) d\tau \quad (13)$$

$$q(t) = \begin{cases} q(t) & t \leq LT \\ 1/2 & t > LT \end{cases} \quad (14)$$

Here  $L$  is the constraint length, which determines the duration of the non-zeros part of  $f(t)$  and the non-constant part of  $q(t)$ . There are various types of frequency pulse functions, such as rectangular shape, raised cosine (RC), and spectrally raised cosine. It can be seemed that the instantaneous frequency is determined by the consecutive  $L$  symbols. At the  $n$ th symbol interval, the instantaneous phase of the  $l$ th data stream of the  $k$ th user can be depicted as

$$\phi_{k,l}(t) = \theta_{k,l}(t, n) + \xi_{k,l}(n-L), \quad nT \leq t < (n+1)T \quad (15)$$

$$\theta_{k,l}(t, n) = 2\pi h \sum_{i=n-(L-1)}^n c_{k,l}(i) q(t-iT) \quad (16)$$

$$\xi_{k,l}(n-L) = [\pi h \sum_{i=-\infty}^{n-L} c_{k,l}(i)] \bmod 2\pi \quad (17)$$

The term  $\theta_{k,l}(t, n)$  represents the instant phase, which is composed by the changing parts of the previous  $L$  symbols. The term  $\xi_{k,l}(n-L)$  is the accumulative phase, which is composed by the non-changing part of all the previous symbols up to the  $(n-L)$ th interval. In the CPM-IA system, the modulation index  $h$  is rational, i.e.,  $h=2q/p$ , where  $p$  and  $q$  are mutual prime numbers. It can be proved that the number of distinct values of  $\xi_{k,l}(n-L)$  is  $p$  [26]. Therefore, we introduce a vector which represents the state of the CPM waveform at  $t=nT$  as

$$\mathbf{\Omega}_{k,l}(n) = [\xi_{k,l}(n-L), c_{k,l}(n-L+1), \dots, c_{k,l}(n-1)] \quad (18)$$

It can be seemed that the state is determined by all the previous symbols, and there are  $p2^{L-1}$  distinct states. Consequently, the information of the previous symbols is imbedded in the phase, which can be utilized to improve the performance of the detector.

### C. The Detection of CPM-IA Scheme

Throughout this paper, it is assumed that the receiver can achieve perfect carrier recover and symbol synchronization. Different from the traditional symbol-by-symbol detectors, the demodulator of CPM signal must take the previous symbols into consideration. To fully explore the memory of CPM-IA scheme, the maximal likelihood sequence detection (MLSD) can be leveraged to achieve optimum detection. The MLSD calculates the likelihood of the received signal  $\hat{S}_{k,l}(t)$  and the local generated waveforms, and selects the local sequence that has the maximal likelihood as the demodulated sequence. This can be achieved by the Viterbi algorithm. The processed received signal  $\hat{S}_{k,l}(t)$  is

first correlated with the local matched filters to generate the branch metric, which will be accumulated by the following Viterbi decoder. The Viterbi decoder can select the optimal path with the maximal likelihood. More details on VA can be found in [26], and it will not be provided due to concision of the paper.

### D. The Low-Complexity Detection of CPM-IA Scheme

The Viterbi algorithm can achieve optimal detection; however, the computational cost of VA is large, posing limits to its applications in the practical networks. The large complexity mainly comes from the large number of matched filters and states of Viterbi decoder. As shown in the previous two subsections, the number of the states of Viterbi decoder is  $p2^{L-1}$ , and the correlation requires as much as  $2^L$  matched filters. Therefore, the computational cost increases exponentially with the constraint length  $L$ .

To reduce the complexity of the demodulator of CPM-IA scheme, a low complexity pulse amplitude modulated decomposition algorithm is introduced to the proposed scheme. According to [27], the CPM waveform can be decomposed by the PAM components as

$$s(t) = \sum_{n=-\infty}^{\infty} \sum_{q=0}^{Q-1} g_{q,n} C_q(t-nT) \quad (19)$$

where  $C_q(t)$  and  $g_{q,n}$  represent the PAM components and the corresponding pseudo-symbols, respectively. The PAM components of the CPM signal with RC frequency pulse function,  $L=3$ , and  $h=2/3$  are depicted in Fig. 2. One important feature of the PAM components is that they vary in duration and signal energy. As shown in Fig. 2, the component  $C_0$  has the largest amplitude and energy, while the amplitudes of  $C_2$  and  $C_3$  are so small that they can be discarded. Therefore, the major PAM components can be leveraged as the matched filters to generate the branch metrics. Since the number of major PAM components is smaller than that of the match filters in the traditional VA, the computational cost can be reduced significantly, without much detection performance loss.

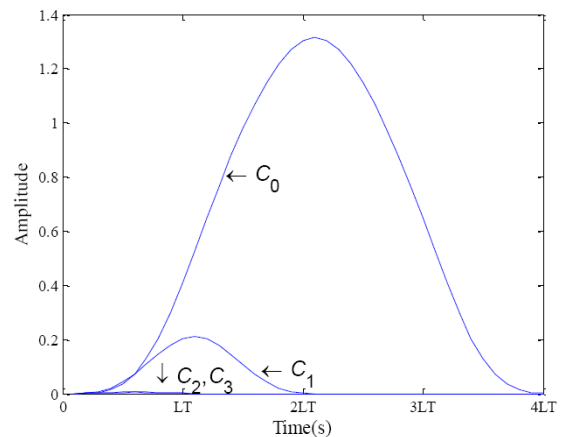


Fig. 2. The PAM components of CPM signal with RC frequency pulse function,  $L=3$ , and  $h=2/3$

## IV. SPATIAL-FREQUENCY DOMAIN CPM-IA SCHEME

The traditional IA system can mitigate the interferences and increase the throughput effectively when the IA feasibility constraint is satisfied. However, as the number of users increases, the spatial alignment might be difficult to achieve. When the number of users exceeds that the traditional IA can afford, the interferences will become strong, degrading the QoS of the communication systems significantly. Against this problem, we proposed a novel special-frequency domain CPM-IA scheme to eliminate the interferences when the IA feasibility constraint cannot be met.

The essential idea of SFD-CPM-IA scheme is to divide the large numbers of users into several groups. As shown in Fig. 3, for the  $(M \times N, d)^K$  networks where  $K > (M+N)/d-1$ , the SFD-CPM-IA scheme will cluster the  $K$  users into  $R$  groups, with  $G$  users in each cluster so that the IA feasibility constraint can be satisfied within each group, i.e.,  $G \leq (M+N)/d-1$ . Therefore, the CPM-IA scheme can be applied to each cluster to mitigate the intra-cluster interference. On the other hand, the users within the  $i$ th group will communicate through central frequency  $f_i$ . Since different groups transmit data through different frequency bands, the interferences from the other groups can be easily eliminated by the front-end band pass filter. More importantly, the bandwidth of each group is relatively narrow since CPM is employed. Consequently, the frequency gap of the adjacent groups can be set to be relatively small as shown in Fig. 4, without interfering with each other. Therefore, the total bandwidth of the SFD-CPM-IA scheme can be reduced due to the high bandwidth efficiency of CPM.

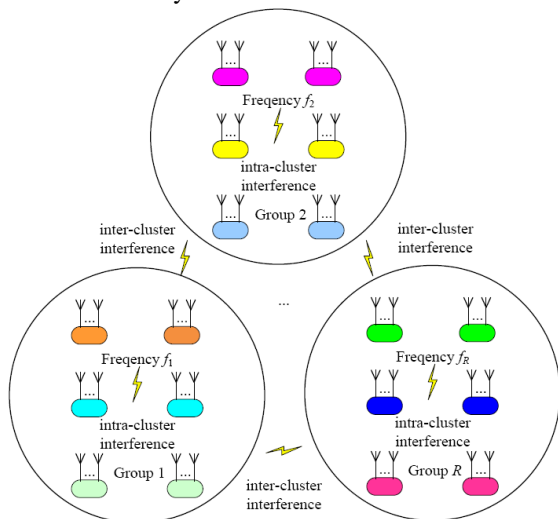


Fig. 3. The SFD-CPM-IA scheme

From the analysis above, it can be seen that the SFD-CPM-IA scheme can not only inherit the high bandwidth efficiency of CPM-IA scheme, but also further eliminate the strong interferences that the traditional IA system cannot handle when the IA feasibility constraint cannot be satisfied. Therefore, the proposed SFD-CPM-IA scheme can accommodate many more users to communicate simultaneously, fulfilling the increasing number of users in modern wireless networks.

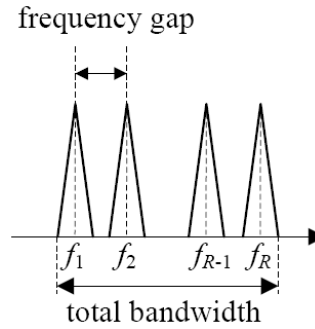


Fig. 4. The frequency bands of SFD-CPM-IA scheme

### V. NUMERICAL RESULTS

In this section, we evaluate the performance of the proposed CPM-IA scheme and compare it with the traditional BPSK-IA system. The power spectrum is compared, and the bit error rate (BER) under different channel configurations is evaluated. Moreover, the proposed SFD-CPM-IA scheme is evaluated in the large scale networks, and compared with the conventional IA system from the perspective of BER. It is assumed that perfect carrier phase and symbol synchronization can be achieved. The frequency pulse function of the CPM signal is chosen to be the raised cosine function with  $L=3$ , and the modulation index is  $h=2/3$ . Therefore, traditional VA requires  $2^L=8$  matched filters.

#### A. Spectrum Comparison

The single side band spectral density of the complex base band signals of BPSK-IA and CPM-IA schemes is depicted in Fig. 5 and Fig. 6, respectively. We randomly generate 4096 equiprobable bits with data rate of 2M bits/sec and sample rate of 32M samples/sec to evaluate the associated spectrum. As reflected in Fig. 5, the spectrum of BPSK-IA scheme occupies a wide bandwidth and the power of the sidelobe attenuates slowly during the bandwidth of  $8 f_b$  from the central frequency. On the contrary, the power of the sidelobe of CPM-IA scheme in Fig. 6 decreases rapidly, and it only takes no more than  $1 f_b$  to reach the level of -120 dB. Therefore, the proposed scheme can reduce the bandwidth of the transmitted signal dramatically.

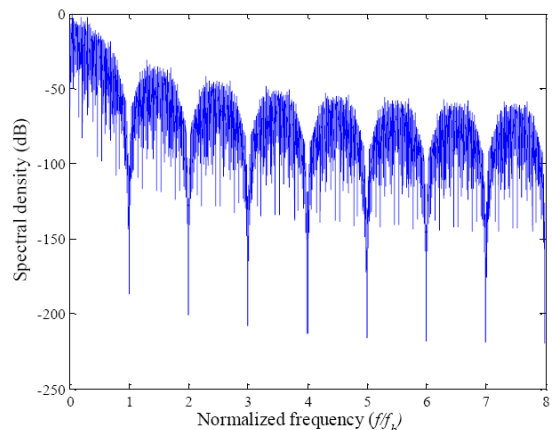


Fig. 5. Spectral density of BPSK-IA scheme

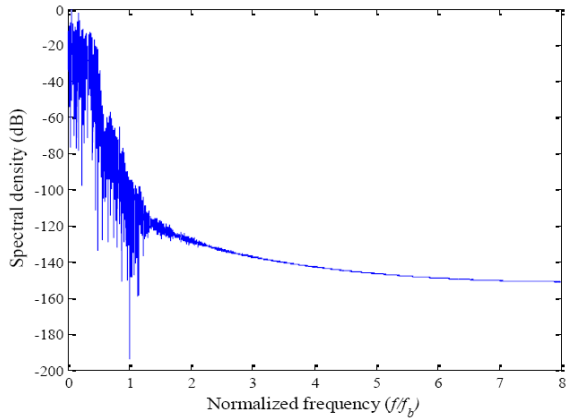


Fig. 6. Spectral density of CPM-IA scheme

**B. Error Performance of CPM-IA Scheme**

The CPM-IA scheme features not only in narrow bandwidth, but also in good BER performance. As shown in Section III, there is memory inherent in the phase of CPM signal, which can provide extra gains to the symbol detection. In this subsection, we evaluate the BER performance of the proposed CPM-IA and the conventional BPSK-IA schemes in Fig. 7 and Fig. 8. Incidentally, as shown in Fig. 2, there are four PAM components which constitute the CPM signal, i.e.,  $C_0$ ,  $C_1$ ,  $C_2$ , and  $C_3$ . In the following simulations, the performance of the low complexity PAM decomposition algorithm is also evaluated, and we consider two cases where the largest one ( $C_0$ ) and two ( $C_0$  and  $C_1$ ) PAM components are leveraged to correlate with the received signal. For each simulation below, the BER is averaged over 100 MIMO channel realizations.

From the results in Fig. 7 for the  $(4 \times 4, 1)^7$  network, the CPM-IA scheme requires lower  $E_b/N_0$  than BPSK-IA system at the same BER. Considering  $BER=10^{-5}$ , the  $E_b/N_0$  required by the proposed scheme is 15 dB, which is 2 dB lower than that of the traditional scheme. As  $E_b/N_0$  increases, the advantage of CPM-IA over BPSK-IA becomes even more significant. Therefore, the memory in CPM-IA scheme can help reducing the  $E_b/N_0$  which is required to reach a certain BER level. When the PAM decomposition is applied to CPM-IA system, the complexity of the demodulator can be reduced. When only one PAM component, i.e.,  $C_0$  is applied, it takes only one matched filter. Although the associated BER is higher than that with VA, its performance is still better than BPSK-IA system. When two PAM components are applied, the associated BER performance is almost the same as that with VA. Therefore, the PAM decomposition algorithm can provide a good tradeoff between the BER performance and computational cost.

The proposed scheme can not only be applied to the single data stream system, but also to the multi data streams scenario. Considering the  $(4 \times 4, 2)^3$  networks in Fig. 8, the BER performance is a little inferior to that in Fig. 7 because of the increase in the number of data streams. In spite of this, the BER of the proposed scheme

is lower than that of the traditional system, especially in the high  $E_b/N_0$  regimes. When  $E_b/N_0=18$  dB is concerned, the corresponding BER of BPSK-IA, CPM-IA with VA, CPM-IA with one PAM component, and CPM-IA with two PAM components is  $1.9 \times 10^{-5}$ ,  $1.0 \times 10^{-6}$ ,  $5.6 \times 10^{-6}$ , and  $1.0 \times 10^{-6}$ , respectively. Therefore, the proposed scheme can achieve better BER performance than the conventional one, and the PAM decomposition algorithm can reduce the complexity without too much performance loss.

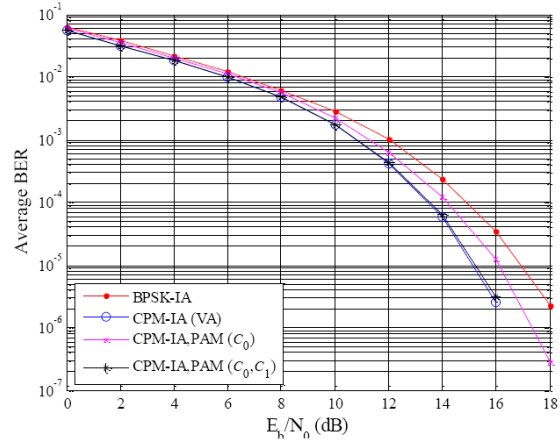


Fig. 7. Average BER of BPSK-IA scheme and CPM-IA schemes with VA and PAM decomposition in the  $(4 \times 4, 1)^7$  channel.

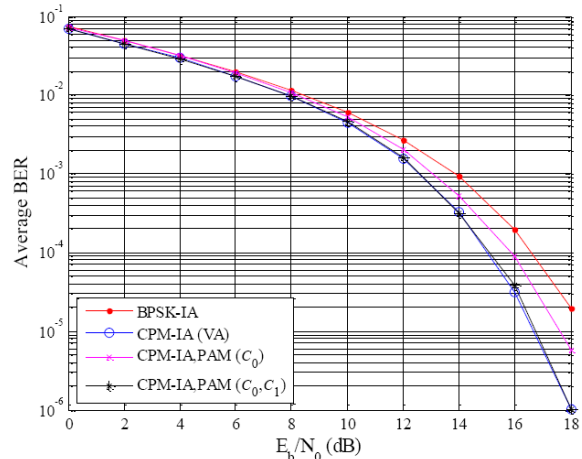


Fig. 8. Average BER of BPSK-IA scheme and CPM-IA schemes with VA and PAM decomposition in the  $(4 \times 4, 2)^3$  channel

**C. Error Performance of SFD-CPM-IA Scheme**

In this subsection, we consider the large scale MIMO networks where the IA feasibility constraint is on longer satisfied. The scenarios of 5 transmitting and receiving antennas are considered in Fig. 9 and Fig. 10 for the  $(5 \times 5, 1)^{27}$  and  $(5 \times 5, 2)^{12}$  networks, respectively. According to the IA feasibility condition, when  $M=N=5$ , the maximal numbers of users that the traditional IA networks can accommodate are 9 and 4 for  $d=1$  and  $d=2$ , respectively. Therefore, the proposed SFD-CPM-IA scheme partitions the users into  $R=3$  groups, which  $G=9$  and  $G=4$  for the  $(5 \times 5, 1)^{27}$  and  $(5 \times 5, 2)^{12}$  channels, respectively. In the simulations below, the performance of the conventional

IA system which employs BPSK is also evaluated. Besides, the PAM decomposition algorithm can also be applied to the SFD-CPM-IA scheme, and the scenarios where one and two PAM components are utilized to approximate the CPM signals are considered.

As shown in Fig. 9, the BER of the conventional BPSK-IA system stays at the unacceptable high level of  $10^{-1}$ , indicating that the interference is so strong and the communication is likely to be terminated. On the contrary, the SFD-CPM-IA scheme can achieve much lower BER, and the associated performance improves as  $E_b/N_0$  increases. For instance, the BER of SFD-CPM-IA scheme at  $E_b/N_0=12$  dB is  $6.6 \times 10^{-7}$ , which is 6 orders lower than that of BPSK-IA system. When the PAM decomposition algorithm is applied, it still exhibits much better performance than the traditional system, and the one which leverages two PAM components can achieve almost the same BER as VA. Although the BER of the PAM decomposition with one PAM component is inferior to VA, the degradation is slight and acceptable.

Similar behavior can be observed in Fig. 10 for the  $(5 \times 5, 2)^{12}$  channel. From the results, it can be seen that the conventional BPSK-IA system still suffers from strong interference and shows poor BER. The SFD-CPM-IA scheme and the associated PAM decomposition algorithm exhibit much better performance. Considering  $E_b/N_0=18$  dB, the BER of BPSK-IA, SFD-CPM-IA with VA, SFD-CPM-IA with one PAM component, and SFD-CPM-IA with two PAM components is  $1.8 \times 10^{-1}$ ,  $3.0 \times 10^{-5}$ ,  $6.2 \times 10^{-5}$ , and  $3.0 \times 10^{-5}$ , respectively.

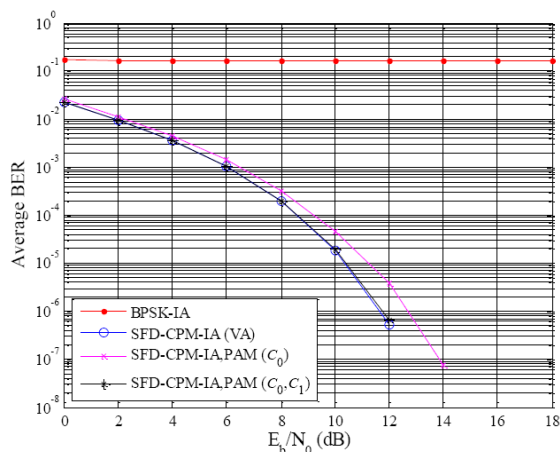


Fig. 9. Average BER of BPSK-IA scheme and SFD-CPM-IA schemes with VA and PAM decomposition in the  $(5 \times 5, 1)^{27}$  channel

## VI. CONCLUSIONS

In this paper, a novel high bandwidth efficiency IA scheme has been proposed, which employs the continuous phase modulation to reduce the signal bandwidth. The precoding and decoding matrices design strategy, the modulator and demodulator of the proposed scheme have been presented. In addition, a low-complexity PAM decomposition algorithm has been introduced to reduce the computational cost of the

receiver. More importantly, a novel spatial-frequency domain CPM-IA scheme has been proposed, which can jointly align the interferences into the spatial and frequency domains so that the massive number of users can transmit data normally even when the IA feasibility constraint is not satisfied. Numerical results have shown that the proposed scheme can achieve better BER performance and much narrower bandwidth than the traditional BPSK-IA scheme. The PAM decomposition algorithm can reduce the number of correlators only with slight BER degradation. In addition, the SFD-CPM-IA scheme can effectively mitigate the interferences and maintain the QoS of the system when the number of users exceeds the IA feasibility condition.

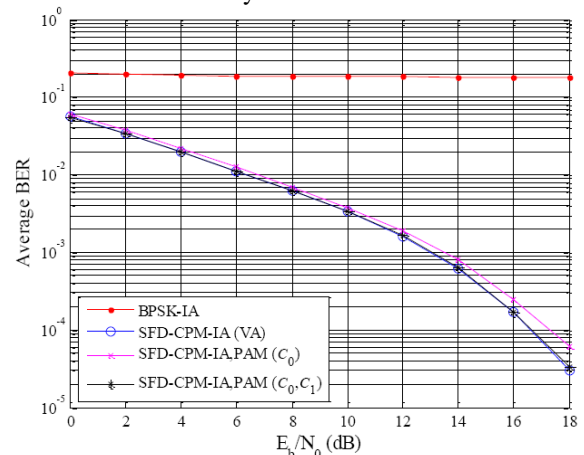


Fig. 10. Average BER of BPSK-IA scheme and SFD-CPM-IA schemes with VA and PAM decomposition in the  $(5 \times 5, 2)^{12}$  channel

## ACKNOWLEDGMENT

We would like to thank the editors for handling this paper. We would also like to thank the reviewers for their detailed reviews and constructive comments, which have helped us to improve the quality of this article.

## REFERENCES

- [1] V. R. Cadambe and S. A. Jafar, "Interference alignment and degrees of freedom of the  $K$ -user interference channel," *IEEE Trans. Inf. Theory*, vol. 54, no. 8, pp. 3425-3441, Aug. 2008.
- [2] H. Sung, S. H. Park, K. J. Lee, and I. Lee, "Linear precoder designs for  $K$ -user interference channels," *IEEE Trans. Wireless Commun.*, vol. 9, no. 1, pp. 291-301, Jan. 2010.
- [3] S. W. Peters and R. W. Heath, "Cooperative algorithms for MIMO interference channels," *IEEE Trans. Veh. Technol.*, vol. 60, no. 1, pp. 206-218, Jan. 2011.
- [4] K. Gomadam, V. R. Cadambe, and S. A. Jafar, "Approaching the capacity of wireless networks through distributed interference alignment," in *Proc. IEEE Global Telecommunications Conference*, 2008, pp. 1-6.
- [5] K. Gomadam, V. R. Cadambe, and S. A. Jafar, "A distributed numerical approach to interference alignment and applications to wireless interference networks," *IEEE Trans. Inf. Theory*, vol. 57, no. 6, pp. 3309-3322, Jun. 2011.
- [6] E. Lu, I. T. Lu, and J. Li, "Interference alignment: A building block of coordinated beamforming transceiver designs," *Journal of Communications*, vol. 6, no. 5, pp. 409-419, Aug. 2011.

[7] O. El Ayach, A. Lozano, and R. W. Heath, "On the overhead of interference alignment: training, feedback, and cooperation," *IEEE Trans. Wireless Commun.*, vol. 11, no. 11, pp. 4192-4203, Nov. 2012.

[8] J. S. Kim, S. H. Moon, S. R. Lee, and L. Inky, "A new channel quantization strategy for MIMO interference alignment with limited feedback," *IEEE Trans. Wireless Commun.*, vol. 11, no. 1, pp. 358-366, Jan. 2012.

[9] N. Zhao, F. R. Yu, and V. C. M. Leung, "Opportunistic communications in interference alignment networks with wireless power transfer," *IEEE Wireless Communications*, in Press

[10] X. Chen, S. H. Song, and K. B. Letaief, "Interference alignment in dual-hop MIMO interference channel," *IEEE Trans. Wireless Commun.*, vol. 13, no. 3, pp. 1274-1283, Mar. 2014.

[11] D. S. Jin, J. S. No, and D. J. Shin, "New interference alignment schemes with full and half-duplex relays for the quasi-static X channel," *IET Communications*, vol. 8, no. 3, pp. 351-359, Feb. 2014.

[12] B. Guler and A. Yener, "Selective interference alignment for MIMO cognitive femtocell networks," *IEEE J. Sel. Areas Commun.*, vol. 32, no. 3, pp. 439-450, Mar. 2014.

[13] Y. Xu and S. W. Mao, "Stackelberg game for cognitive radio networks with MIMO and distributed interference alignment," *IEEE Trans. Veh. Technol.*, vol. 63, no. 2, pp. 879-892, Feb. 2014.

[14] J. Yoon, W. Y. Shin, and H. S. Lee, "Energy-efficient opportunistic interference alignment," *IEEE Commun. Lett.*, vol. 18, no. 1, pp. 30-33, Jan. 2014.

[15] J. Mao, G. Xie, J. Gao, and Y. Liu, "Energy efficiency optimization for cognitive radio MIMO broadcast channels," *IEEE Commun. Lett.*, vol. 17, no. 2, pp. 337-340, Feb. 2013.

[16] H. Zhang, C. Jiang, N. C. Beaulieu, X. Chu, X. Wen, and M. Tao, "Resource allocation in spectrum-sharing OFDMA femtocells with heterogeneous services," *IEEE Trans. Commun.*, vol. 62, no. 7, pp. 2366-2377, Jul. 2014.

[17] C. Jiang, H. Zhang, Y. Ren, and H. H. Chen, "Energy-efficient non-cooperative cognitive radio networks: micro, meso, and macro views," *IEEE Commun. Mag.*, vol. 52, no. 7, pp. 14-20, Jul. 2014.

[18] N. Zhao, F. R. Yu, H. Sun, A. Nallanathan, and H. Yin, "A novel interference alignment scheme based on sequential antenna switching in wireless networks," *IEEE Trans. Wireless Commun.*, vol. 12, no. 10, pp. 5008-5021, Oct. 2013.

[19] E. Hosseini and E. Perrins, "Timing, carrier, and frame synchronization of burst-mode CPM," *IEEE Trans. Commun.*, vol. 61, no. 12, pp. 5125-5138, Dec. 2013.

[20] L. Bing and B. M. Bai, "Design of simplified maximum-likelihood receivers for multiuser CPM systems," *Scientific World Journal*, Jan. 2014.

[21] G. Thakur, "Spread spectrum codes for continuous-phase modulated systems," *IEEE Trans. Commun.*, vol. 62, no. 3, pp. 952-960, Mar. 2014.

[22] B. F. Beidas, S. Cioni, U. De Bie, A. Ginesi, R. Iyer-Seshadri, P. Kim, *et al.*, "Continuous phase modulation for broadband satellite communications: design and trade-offs," *International Journal of Satellite Communications and Networking*, vol. 31, no. 5, pp. 249-262, Sep. 2013.

[23] T. F. Detwiler, S. M. Searcy, S. E. Ralph, and B. Basch, "Continuous phase modulation for fiber-optic links," *Journal of Lightwave Technology*, vol. 29, no. 24, pp. 3659-3671, Dec. 2011.

[24] S. Saleem and G. L. Stuber, "Trellis termination of multi-h CPM and the diophantine frobenius problem," *IEEE Trans. Commun.*, vol. 59, no. 8, pp. 2196-2205, Aug. 2011.

[25] S. Chen and R. S. Cheng, "Clustering for interference alignment in multiuser interference network," *IEEE Trans. Veh. Technol.*, vol. 63, no. 6, pp. 2613-2624, Jul. 2014.

[26] F. Xiong, *Digital Modulation Techniques*, 1st ed. Artech House, UK: London, 2000, pp. 259-337.

[27] G. Cariolaro, "A system-theory approach to decompose CPM signals into PAM waveforms," *IEEE Trans. Commun.*, vol. 58, no. 1, pp. 200-210, Jan. 2010.



**Zhilu Wu** is a professor in the School of Electronics and Information Engineering and the dean of the Information Engineering Department at Harbin Institute of Technology (HIT), Harbin, China. He received the B.S. degree in electronic instrument and measurement technology in 1983, M.E. degree in signal and information processing in 1989, and Ph.D. in information and communication engineer in 2008, respectively, from HIT. His research interests include wireless communication, interference alignment, software radio, and artificial neural network.



**Lihui Jiang** received the B.S. degree in science and technology of optical information in 2009 from South China University of Technology, Guangzhou, China. He received the M.E. degree in signal and information processing in 2011 from HIT. He is currently working toward the Ph.D. degree in information and communication at HIT. His research interests include wireless communication, interference alignment, and continuous phase modulation.



**Guanghui Ren** is a professor in the School of Electronics and Information Engineering at HIT. He received the B.S. degree in electronic instrument and measurement technology in 1984 and M.E. degree in signal and information processing in 2003 from HIT. His research interests include wireless communication, interference alignment, image processing, automatic test systems, and parallel computing.



**Gangyi Wang** is currently a lecturer in the School of Instrumentation Science and Opto-electronics Engineering at Beihang University, Beijing, China. He received the B.S. degree in electronics and information engineering in 2006, the M.E. degree and Ph.D. degree in information and communication engineering in 2008 and 2013, respectively, from HIT. His research interests include computer vision, interference alignment, and embedded systems.